

Debye-Hückel theory for spin ice at low temperature

C. Castelnovo^{1,2}, R. Moessner³, and S. L. Sondhi⁴

¹ *Rudolf Peierls Centre for Theoretical Physics, University of Oxford, Oxford, OX1 3NP, United Kingdom*

² *SEPNET and Hubbard Theory Consortium, Department of Physics, Royal Holloway University of London, Egham TW20 0EX, United Kingdom*

³ *Max-Planck-Institut für Physik komplexer Systeme, Dresden, 01187, Germany and*

⁴ *Department of Physics, Princeton University, Princeton, NJ 08544, USA*

(Dated: September 11, 2018)

At low temperatures, spin ice is populated by a finite density of magnetic monopoles—pointlike topological defects with a mutual magnetic Coulomb interaction. We discuss the properties of the resulting magnetic Coulomb liquid in the framework of Debye Hückel theory, for which we provide a detailed context-specific account. We discuss both thermodynamical and dynamical signatures, and compare Debye Hückel theory to experiment as well as numerics, including data for specific heat and AC susceptibility. We also evaluate the entropic Coulomb interaction which is present in addition to the magnetic one and show that it is quantitatively unimportant in the current compounds. Finally, we address the role of bound monopole anti-monopole pairs and derive an expression for the monopole mobility.

I. INTRODUCTION

Spin systems with long-range interactions, where each spin interacts with all others, present a formidable challenge to theoretical analysis. While simplifications occur in the limit of infinite range interactions, the case of dipolar interactions in three spatial dimensions is particularly complex due to their (non-integrable) algebraic decay combined with angular dependence on the spin direction¹. As the determination of the behaviour of even a spin model with only short ranged competing interactions can pose a non-trivial problem, it is a priori not obvious how long-range interactions can be treated.

A remarkable counterexample to this case for pessimism is provided by spin ice², a dipolar Ising magnet on the pyrochlore lattice that fails to order down to the lowest temperatures accessed. To a fine approximation, which we detail below, spin ice is governed by a model dipolar Hamiltonian about which quite a lot is known,

$$H = J_{\text{ex}}^{\text{nn}} \sum_{\langle ij \rangle} \mathbf{S}_i \cdot \mathbf{S}_j + \frac{\mu_0}{4\pi} \sum_{i < j} \left[\frac{\mathbf{S}_i \cdot \mathbf{S}_j}{r_{ij}^3} - \frac{3(\mathbf{S}_i \cdot \mathbf{r}_{ij})(\mathbf{S}_j \cdot \mathbf{r}_{ij})}{r_{ij}^5} \right],$$

where $J_{\text{ex}}^{\text{nn}}$ is the exchange interaction truncated at the nearest-neighbour level, the spins \mathbf{S}_i point parallel to the local [111] axis (see Fig. 1), and μ_0 is the vacuum permeability. The rare earth spins \mathbf{S}_i have typically a dipole moment of approximately $10 \mu_B$ ($\mu_B = \text{Bohr magneton}$).

Most prominently, the model Hamiltonian has an extensive set of ground states which can be specified by a purely local “ice rule”. Their entropy is known to an excellent approximation due to Pauling’s work already in the context of water ice and it has been observed experimentally³. The $T \rightarrow 0$ static correlations are averages over this ground state manifold and their long distance forms are known as they are described by an emergent gauge field in the Coulomb phase⁴⁻⁸, which have also been observed experimentally⁹⁻¹¹.

At low temperatures the physics of the system turns out to allow a further simplification. The excitations about the

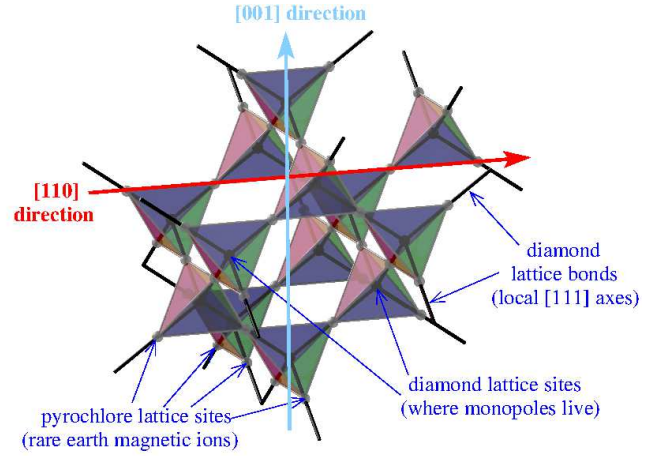


FIG. 1. The magnetic moments in spin ice reside on the sites of the pyrochlore lattice, which consists of corner sharing tetrahedra. These sites are at the same time the midpoints of the bonds of the diamond lattice (black) defined by the centres of the tetrahedra. The Ising axes are the local [111] directions, which point along the respective diamond lattice bonds. The bonds of the pyrochlore lattice are in the [110] directions, while a line joining the two midpoints of opposite bonds on the same tetrahedron defines a [100] direction.

ground state manifold take the form of magnetic monopoles—pointlike defects that interact via a magnetic Coulomb interaction energy which is independent of the background spin state¹². In this regime, the magnetic monopoles are sparse, as their number is suppressed on account of their excitation gap. This in turn has two implications. Firstly, the static correlators continue to be dominated by their known $T = 0$ forms up to the inter-monopole separation, whereupon they match onto the asymptotics of the paramagnetic phase¹³. Secondly, the low temperature thermodynamics of spin ice can be transformed from that of a dense set of *localised* dipolar spins to that of a dilute set of *itinerant* Coulombically interacting particles—a (magnetic) Coulomb liquid as first noted

in Ref. 12:

$$H = \frac{\mu_0}{4\pi} \sum_{i < j} \frac{q_i q_j}{r_{ij}} + \Delta \sum_i \left(\frac{q_i}{2\mu/a_d} \right)^2,$$

where the charges q_i take the values $\pm 2\mu/a_d$, $\mu \simeq 10\mu_B$ being the dipole moment of a spin and a_d the distance between the centres of adjacent tetrahedra (diamond lattice constant in Fig. 1), and Δ is the energy cost of a monopole.

The transformation is extremely helpful as much is known about Coulomb liquids, with a venerable history spanning fields from statistical physics all the way to the chemistry of electrolytes. Indeed, the known properties of the Coulomb liquid have led to an explanation of the ‘liquid-solid’ phase transition of spin ice in a [111] field¹², as well as of its magnetic specific heat¹⁰ in zero field. More recently, much attention has been devoted to the study of the ‘magnetricity’¹⁴ in these ‘magnetolytes’¹⁵, the equilibrium and non-equilibrium behaviour of such a magnetic Coulomb liquid, inspired by the analogous electric phenomena such as the Wien effect^{14,16}.

In this paper, expanding on our previous work in Ref. 10, we develop a low-energy theory for spin ice in the framework of the Debye-Hückel (DH) theory of a dilute Coulomb liquid. DH theory will be familiar to readers from many different disciplines but to our knowledge has never been applied to a three-dimensional magnetic material before the advent of spin ice.

The purpose of this paper is two-fold. First, it gives a detailed and context-specific account of the DH theory for spin ice. Second, its ability to model experimental data is underlined. In particular, we show that an existing framework to describe the dynamics of spin ice, when supplemented by DH theory, provides improved agreement with existing experimental and numerical data on the AC-susceptibility of spin ice^{17–21}.

This is perhaps as good a point as any to digress and address the concerns of readers who may be worried that our replacement of spins by monopoles is too good to be true. Here three points are in order. First, as we have already noted above, the spins do enter the static correlations but in a manner that is understood. Second, a given monopole configuration can be ‘dressed’ by many spin configurations. However summing over these dressings generates an effective entropic Coulomb attraction between the monopoles at long wavelengths (see e.g., Ref. 22) which can *also* be included in the Coulomb/DH framework. We will address this point in Sec. V and find that the entropic effect can be ignored for the present set of spin ice compounds. Third, there is still a remaining issue that not all monopole configurations are in fact compatible with some spin configuration, and moreover the spins can induce non-trivial structure to the monopole energy landscape which in turn can significantly alter dynamical properties of spin ice out of equilibrium²³. However, these are weak constraints on the Coulomb framework and it seems highly unlikely that they play any role in determining equilibrium properties.

We close the introduction by remarking on the range of applicability of the Coulomb liquid/DH theory framework in the actual compounds (see Fig. 2). At high temperatures, above a

scale T_p , we are in a conventional paramagnetic regime where the monopoles are dense. Below T_p the monopoles become sufficiently dilute that they can be treated by DH theory. At a much lower temperature T_d , the Coulomb phase is unstable to ordering transitions^{24–26}, the details of which are not entirely settled. For the model Hamiltonian, $T_d \equiv 0$. While the Coulomb liquid framework should thus apply in the range $T_d < T < T_p$, the equilibrium DH treatment runs into problems around a temperature $T_f > T_d$ where the system falls out of equilibrium before any ordering is visible. Much of the interest in the spin ice compounds $\text{Dy}_2\text{Ti}_2\text{O}_7$ and $\text{Ho}_2\text{Ti}_2\text{O}_7$ derives from the fact that $T_d, T_f < T_p$, so that there is a window where Coulomb physics is well visible.

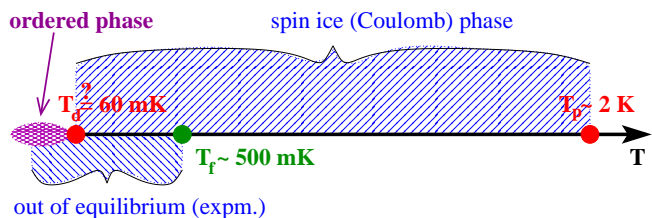


FIG. 2. Schematic illustration of the different temperature regimes in spin ice, separated by T_d , T_f , and T_p as explained in the text. The putative ordering below T_d appears to be prevented by freezing of the magnetic degrees of freedom below T_f , as evidenced e.g., by a discrepancy between field-cooled and zero-field-cooled magnetisation. At temperatures of about T_p , the materials cross over to a trivial paramagnetic behaviour.

The remainder of this paper is organised as follows: we first provide DH background, discuss specificities of its application in the spin ice setting, discuss its range of validity and finally apply it to experiment. In addition, we discuss two other topics of import in this context. Firstly, we determine the size of the entropic Coulomb interaction between monopoles. Secondly, we compute the low-temperature mobility of magnetic monopoles in spin ice with a single-spin flip dynamics believed to be appropriate for experimental compounds $\text{Dy}_2\text{Ti}_2\text{O}_7$ and $\text{Ho}_2\text{Ti}_2\text{O}_7$.

II. DEBYE-HÜCKEL FREE ENERGY

We now turn to the application of DH theory to spin ice. The reader not interested in details of the formalism can skip ahead to Section IV.

A. Non-interacting monopoles

To lay the foundation, let us start by considering the simple case of non-interacting monopoles, corresponding to a nearest-neighbour spin ice model. Since the monopole description of spin ice is valid only when the density of defective tetrahedra is sufficiently small, i.e., at low temperatures, we consider only the less costly defects (3in-1out and 3out-1in

tetrahedra) and neglect charge 2 excitations altogether (4in-Out and 4out-0in) as they cost four times as much energy. The internal energy U of the system is thus proportional to the number of monopoles N ,

$$U = N\Delta = N_t \rho \Delta, \quad (2.1)$$

where Δ is the energy cost of an isolated monopole (assumed in the following to be measured in Kelvin) and $\rho \equiv N/N_t$ is the monopole density per tetrahedron.

The number of configurations that an ensemble of $N/2$ positive (hard-core) monopoles and $N/2$ negative ones can take on a lattice of N_t sites (N_t being the total number of tetrahedra in the system) is given by

$$W = \binom{N_t}{N/2, N/2, (N_t - N)}. \quad (2.2)$$

Using Stirling's approximation in the large N_t and large N limit, we obtain the $\mathcal{S} = k_B \ln W$ 'entropy of mixing',

$$\begin{aligned} S &\equiv \mathcal{S}/k_B \\ &= -N_t [2(\rho/2) \ln(\rho/2) + (1 - \rho) \ln(1 - \rho)] \end{aligned} \quad (2.3)$$

with a concomitant free energy per spin

$$\frac{F_{\text{nn}}}{N_s k_B} = \frac{U - TS}{N_s} \quad (2.4)$$

where the number of spins is twice the number of tetrahedra, $N_s = 2N_t$. Minimizing with respect to ρ , we obtain the known expression for the total monopole density

$$\rho_{\text{nn}} = \frac{2 \exp(-\Delta/T)}{1 + 2 \exp(-\Delta/T)}. \quad (2.5)$$

For small T , and hence small ρ_{nn} , $\rho_{\text{nn}} \simeq 2 \exp(-\Delta/T)$. For large T , Eq. (2.5) tends asymptotically to the value $2/3$, which is clearly incorrect – as expected since random Ising spins on a pyrochlore lattice yield a density $\rho_{\text{random}} = 5/8$ of defective tetrahedra. This can be seen e.g., if we consider a single tetrahedron: out of the $2^4 = 16$ allowed Ising configurations, only 6 satisfy the 2in-2out condition and the remaining 10 configurations violate charge neutrality.

B. Debye-Hückel contribution

One of the major approximations in Sec. II A is the fact that the long range Coulomb interactions between the monopoles were entirely neglected¹². Taking advantage of the analogy between spin ice defects and a two-component Coulomb liquid (in the absence of applied magnetic fields), we can use the Debye approximation to estimate the magnetostatic contribution to the free energy (in degrees Kelvin per spin):²⁷

$$\begin{aligned} \frac{F_{\text{el}}}{N_s k_B} &= -\frac{NT}{4N_s \pi \rho_V a_d^3} \left[\frac{(a_d \kappa)^2}{2} - (a_d \kappa) + \ln(1 + a_d \kappa) \right] \\ \kappa &= \sqrt{\frac{\mu_0 q^2 \rho_V}{k_B T}}, \end{aligned} \quad (2.6)$$

where $\rho_V = N/V$ is the dimensionful volume density of monopoles and a_d is the distance between the centres of two neighbouring tetrahedra (i.e., the dual diamond lattice constant).

It is convenient to express the dimensionless quantity $a_d \kappa$ in terms of the Coulomb energy between two neighbouring monopoles $E_{\text{nn}} \equiv \mu_0 q^2 / (4\pi a_d k_B)$,

$$a_d \kappa = \sqrt{4\pi} \sqrt{\frac{E_{\text{nn}}}{T}} (\rho_V a_d^3). \quad (2.7)$$

Here q stands for the magnitude of the monopole charge ($q = 2\mu/a_d$, where μ is the rare earth magnetic moment¹²).

There are 8 diamond lattice sites in a 16-spin cubic unit cell of side $(4/\sqrt{3}) a_d$. The total volume of the system can then be written as $V = (N_t/8)(4/\sqrt{3})^3 a_d^3$ and

$$\rho_V a_d^3 = \frac{N}{V/a_d^3} = \frac{3\sqrt{3}}{8} \rho. \quad (2.8)$$

As a result, we arrive at

$$\frac{F_{\text{el}}}{N_s k_B} = -\frac{T}{3\sqrt{3}\pi} \left[\frac{(a_d \kappa)^2}{2} - (a_d \kappa) + \ln(1 + a_d \kappa) \right] \quad (2.9)$$

$$a_d \kappa = \sqrt{\frac{3\sqrt{3}\pi E_{\text{nn}}}{2T}} \sqrt{\rho} \equiv \alpha(T) \sqrt{\rho}, \quad (2.10)$$

where the last equation defines the function $\alpha(T)$. In the low temperature limit, the magnetostatic contribution scales as $\rho^{3/2}$, namely

$$\begin{aligned} \frac{F_{\text{el}}}{N_s k_B} &\simeq -\frac{T}{3\sqrt{3}\pi} \frac{(a_d \kappa)^3}{3} \\ &\simeq -\sqrt{\frac{\pi}{8\sqrt{3}}} E_{\text{nn}} \sqrt{\frac{E_{\text{nn}}}{T}} \rho^{3/2}. \end{aligned} \quad (2.11)$$

We can then combine Eqs. (2.9) and (2.10) with Eq. (2.4) from Sec. II A to obtain a mean field free energy – per spin in degrees Kelvin – of an ensemble of N monopoles on a lattice with long range Coulomb interactions:

$$\begin{aligned} \frac{F}{N_s k_B} &= \frac{\rho}{2} \Delta + \frac{T\rho}{2} \ln\left(\frac{\rho/2}{1-\rho}\right) + \frac{T}{2} \ln(1-\rho) \\ &\quad - \frac{T}{3\sqrt{3}\pi} \left\{ \frac{\alpha^2(T)\rho}{2} - \alpha(T)\sqrt{\rho} + \ln[1 + \alpha(T)\sqrt{\rho}] \right\} \\ \alpha(T) &= \sqrt{\frac{3\sqrt{3}\pi E_{\text{nn}}}{2T}}. \end{aligned} \quad (2.12)$$

Note that this reduces to the non-interacting limit if we set $E_{\text{nn}} = 0$.

Minimizing with respect to the defect density ρ , one obtains a self-consistent set of equations:

$$\begin{aligned} \frac{d(F/N_s k_B)}{d\rho} &= \Delta + T \ln\left(\frac{\rho/2}{1-\rho}\right) - \frac{E_{\text{nn}}}{2} \frac{\alpha(T)\sqrt{\rho}}{1 + \alpha(T)\sqrt{\rho}} = 0 \\ \rho &= \frac{2 \exp\left[-\left(\frac{\Delta}{T} - \frac{E_{\text{nn}}}{2T} \frac{\alpha\sqrt{\rho}}{1 + \alpha\sqrt{\rho}}\right)\right]}{1 + 2 \exp\left[-\left(\frac{\Delta}{T} - \frac{E_{\text{nn}}}{2T} \frac{\alpha\sqrt{\rho}}{1 + \alpha\sqrt{\rho}}\right)\right]}. \end{aligned} \quad (2.13)$$

Unfortunately, Eq. (2.13) cannot be solved analytically and one has to resort to numerical methods to obtain $\rho(T)$. We find that the recursive approach

$$\begin{aligned} \rho_0 = \rho_{\text{nn}} &= \frac{2 \exp(-\Delta/T)}{1 + 2 \exp(-\Delta/T)} \\ \rho_{\ell+1} &= \frac{2 \exp \left[- \left(\frac{\Delta}{T} - \frac{E_{\text{nn}}}{2T} \frac{\alpha \sqrt{\rho_\ell}}{1 + \alpha \sqrt{\rho_\ell}} \right) \right]}{1 + 2 \exp \left[- \left(\frac{\Delta}{T} - \frac{E_{\text{nn}}}{2T} \frac{\alpha \sqrt{\rho_\ell}}{1 + \alpha \sqrt{\rho_\ell}} \right) \right]} \end{aligned} \quad (2.14)$$

converges with acceptable accuracy in less than 5 iterations. Substituting $\rho \equiv \rho_{\ell \rightarrow \infty} \simeq \rho_5$ into Eq. (2.12) we obtain numerically the approximate free energy of dipolar spin ice as a function of temperature.

Between Eqns. (2.12) and (2.13) we have obtained the free energy for monopoles in the DH approximation. From this one can compute several thermodynamic quantities of interest (see e.g., Sec. VIA).

III. SPIN ICE PARAMETERS AND DH INTERNAL CONSISTENCY

We first derive the parameters describing the $\text{Dy}_2\text{Ti}_2\text{O}_7$ and $\text{Ho}_2\text{Ti}_2\text{O}_7$ spin ices within the dumbbell model¹² in the subsequent subsection. Following the determination of the parameters, we discuss the range of temperatures over which the treatment is valid.

A. Spin ice parameters in the dumbbell model

The usefulness of the dumbbell model lies in the fact that it correctly captures the long-distance form of the dipolar interaction – as well as the magnetic Coulomb interaction between the monopoles – while preserving the degeneracy of the spin ice states. At the same time, a model of such simplicity cannot do justice to the full short-distance structure of the interactions present in the real compound, which include further-neighbour superexchange as well as quadrupolar interaction terms between the spins. We will thus find in the following sections that the best fit to both numerics and experiment requires slight adjustments to the dumbbell model parameters to obtain quantitatively optimal fits.

We also take this opportunity to caution the reader that the ‘microscopic’ parameters themselves are subject to change on the level of a few percent as experiments and their detailed numerical modeling evolve (and, hopefully, improve) over time. Such changes can be innocuous (e.g. a 1% change to the diamond lattice constant) but since some of the resulting physics is rather delicate, they can feed through to relatively larger corrections, most prominently as a factor 3 in the estimated value of T_d .^{125,26}

From the pyrochlore lattice constant $a = 3.54 \text{ \AA}$ one obtains the diamond lattice constant $a_d = \sqrt{3/2} a = 4.34 \text{ \AA}$. Combined with the spin magnetic moment $\mu = 10\mu_B$ ($\mu_B = 9.27 \cdot 10^{-24} \text{ J/Tesla}$), this gives the monopole charge $q \simeq$

$4.6 \mu_B/\text{\AA} \simeq 4.28 \cdot 10^{-13} \text{ J/(Tesla m)}$ (see Ref. 12 and Supplementary Information therein).

Inserting the dipolar coupling constant

$$D = \frac{\mu_0}{4\pi k_B} \frac{\mu^2}{a^3} \simeq 1.41 \text{ K}$$

($\mu_0/4\pi = 10^{-7} \text{ N/A}^2$, $k_B = 1.38 \cdot 10^{-23} \text{ J/K}$) and the nearest-neighbour exchange coupling $J \simeq -3.72 \text{ K}$ for $\text{Dy}_2\text{Ti}_2\text{O}_7$ ($J \simeq -1.56 \text{ K}$ for $\text{Ho}_2\text{Ti}_2\text{O}_7$) into the expression for the bare cost of a single isolated monopole in Ref. 12, we obtain

$$\begin{aligned} \Delta &= \frac{1}{2} v_0 q^2 = \frac{2J}{3} + \frac{8}{3} \left[1 + \sqrt{\frac{2}{3}} \right] D \\ &= \begin{cases} 4.35 \text{ K} & \text{for Dy}_2\text{Ti}_2\text{O}_7 (J = -3.72 \text{ K}) \\ 5.79 \text{ K} & \text{for Ho}_2\text{Ti}_2\text{O}_7 (J = -1.56 \text{ K}) \end{cases} \end{aligned} \quad (3.1)$$

The energy of two monopoles at nearest neighbour distance is:

$$E_{\text{nn}} = \frac{\mu_0}{4\pi k_B} \frac{q^2}{a_d} \simeq 3.06 \text{ K}. \quad (3.2)$$

Therefore, the creation of two neighbouring monopoles by a single spin flip event in a spin ice configuration where all tetrahedra satisfy the 2in-2out rules incurs an energy cost

$$\Delta_s = 2\Delta - E_{\text{nn}} \simeq \begin{cases} 5.64 \text{ K} & \text{for Dy}_2\text{Ti}_2\text{O}_7 \\ 8.52 \text{ K} & \text{for Ho}_2\text{Ti}_2\text{O}_7 \end{cases}. \quad (3.3)$$

As a final remark, it is interesting to compare the force between two monopoles at nearest neighbour distance,

$$F_{\text{nn}} = \frac{\mu_0}{4\pi} \frac{q^2}{a_d^2} \simeq 9.74 \cdot 10^{-14} \text{ N}, \quad (3.4)$$

to that between two electrons at the same distance, $F_{\text{el}} \simeq 1.22 \cdot 10^{-9} \text{ N}$, four orders of magnitude stronger! By contrast, a pair of Dirac monopoles would experience a force of almost 10^{-5} N .

B. Internal consistency: screening length vs. monopole separation and lattice constant

The Debye screening length ξ_{Debye} is given by the inverse of the constant κ in Eq. (2.10). In units of the diamond lattice constant a_d this amounts to

$$\frac{\xi_{\text{Debye}}}{a_d} = \frac{1}{a_d \kappa} = \sqrt{\frac{2T}{3\sqrt{3}\pi E_{\text{nn}}}} \frac{1}{\sqrt{\rho}}. \quad (3.5)$$

The dependence of ξ_{Debye}/a_d on temperature, after substituting $\rho(T)$ from the numerical solution of Eq. (2.13) is illustrated in Fig. 3 (using for instance $\Delta = 4.7 \text{ K}$).

We anticipate here that there is a systematic discrepancy between the DH approximation and the MC simulation results on the heat capacity for $T \gtrsim 1 \text{ K}$ (see Fig. 7). To understand this, we note the following.

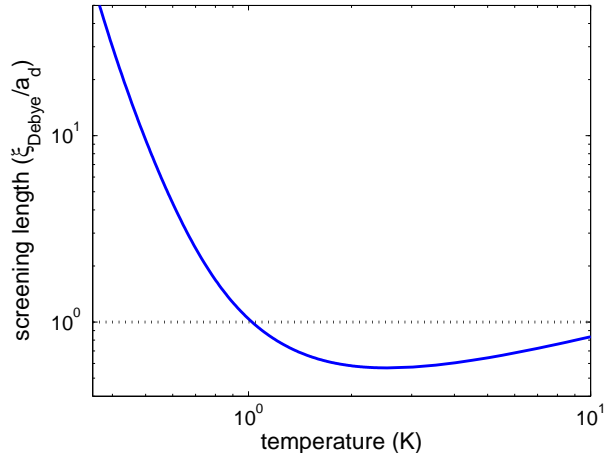


FIG. 3. Plot of the Debye screening length vs temperature, using the density from the numerical solution to the Debye-Hückel calculation in Sec. II B.

Firstly, above $T \simeq 1$ K the screening length becomes shorter than the lattice spacing. This artefact arises because the DH term in the free energy was derived in the continuum. For $T \gtrsim 1$ K one thus needs to consider the DH results with caution. Having said this, once the screening length gets very short, the long range nature of the Coulomb interaction becomes less important. One can then reliably truncate the interactions to short range and use alternative approaches to compute the free energy and other thermodynamic quantities, as illustrated for instance in Appendix A.

Secondly, as T approaches the Curie-Weiss temperature of about 2K, the average separation between monopoles, $d \sim a_d \rho^{-1/3}$, becomes comparable to the lattice constant a_d and the monopole picture is no longer appropriate to describe spin ice – monopoles are useful as long as they are sparse, otherwise it is more efficient to work directly with the microscopic spin degrees of freedom. (In addition, for even higher values of T , the neglect of doubly-charged monopoles becomes problematic.) For instance, it would be more appropriate to use a conventional high-temperature series expansion.

Another parameter of physical relevance is the ratio of screening length to monopole separation: the larger this ratio, the more appropriate a continuum description is. The dimensionful monopole density ρ_V can be expressed in terms of the monopole density per tetrahedron ρ (which appears in the DH calculations in Sec. II) using the relation $\rho_V = 3\sqrt{3}\rho/(8a_d^3)$. From it, we can obtain the average monopole separation $\rho_V^{-1/3}$. By comparing these two length scales, one observes that DH theory is near an ‘internal’ limit of validity, as the ratio $\xi_{\text{Debye}}/\rho_V^{-1/3}$ is close to one throughout the range of interest. Indeed, $\xi_{\text{Debye}}/\rho_V^{-1/3} \gtrsim 1$ only below 300 mK, dropping by a factor three towards its minimum at 1 K (not shown).

C. Role of the magnetostatic contribution

It is interesting to quantify how big the change brought about by the DH accounting of Coulomb interactions and screening actually is. To do this, let us consider the density of monopoles, which will play a role later in the comparison with Monte Carlo simulation results (Sec. IV A). In Fig. 4 we plot the ratio of the monopole densities from Sec. II B with and without the magnetostatic contribution Eq. (2.9), using parameters appropriate for spin ice $\text{Dy}_2\text{Ti}_2\text{O}_7$. Within the re-

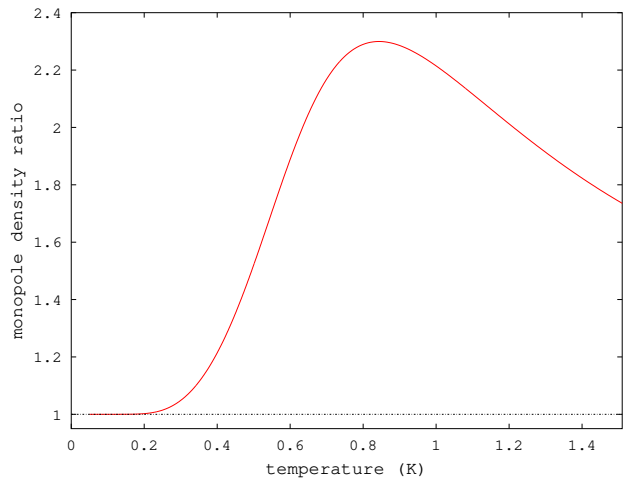


FIG. 4. Ratio of the monopole densities from Sec. II B obtained with and without the Debye-Hückel magnetostatic contribution, Eq. (2.9), as a function of temperature.

gion $T \lesssim 1$ K, one notices that DH theory can lead to a more than two-times larger monopole density. Given that spin ice materials are prone to falling out of equilibrium at temperatures $T \lesssim 0.5$ K, the behaviour of the system in the temperature window where DH corrections are sizeable is of crucial relevance to experiment. In the limit of low temperatures, the DH correction instead becomes less and less important.

D. Monopole-antimonopole pairing

Debye-Hückel theory neglects the association of monopoles into neutral dipolar pairs (see Ref. 31 and references therein). Although this can in general lead to sizeable discrepancies between DH predictions and experiments, we argue hereafter that pairing corrections are small for the observables in spin ice that we consider here, due to the combination of its limit of validity ($T \lesssim 1$ K, see Sec. III B) and the relatively larger energy cost for a monopole excitation, $\Delta \sim 4 - 5$ K, in comparison to the Coulomb energy when hard core charges come into ‘contact’ (nearest-neighbour distance), $E_{\text{nn}} \simeq 3.06$ K.

In order to show this, let us assume that monopoles in spin ice are either free (density ρ_0), if separated by a distance larger than ℓ_B , or bound in a pair, if separated by a distance d shorter

than ℓ_B . Here we choose ℓ_B to equal the Bjerrum length, at which the thermal energy $k_B T$ equals the Coulomb energy:

$$\ell_B/a_d = \frac{\mu_0}{4\pi a_d} \frac{(2\mu/a_d)^2}{2k_B T} \simeq \frac{1.54}{T[\text{K}]} \quad \text{for Dy}_2\text{Ti}_2\text{O}_7, \quad (3.6)$$

We now consider only Coulomb interactions amongst free monopoles and between the two monopoles belonging to the same pair, while we neglect monopole-pair and pair-pair interactions, on the grounds that they are generally weaker and they decay faster with distance. We also neglect excluded volume effects (therefore, any results we obtain ought to be treated with care as the density of monopoles approaches unity, which is anyway not the regime we are interested in).

The free energy f_0 for the fraction of free monopoles in the system is straightforwardly given by Eq. 2.12. The potential energy term for the bound pairs, of densities ρ_d , $d = 1, 2, \dots, \ell_B$, is also immediate to write as it involves only the inter-pair Coulomb term: $(2\Delta - E_d)\rho_d$, where $E_d \sim E_{\text{nn}}/d$. The entropic contribution to the free energy of a bound pair of characteristic distance d can be computed from the numbers of ways that such pair can appear on the lattice,

$$W = \binom{N_t}{N_t \rho_d} v_d^{N_t \rho_d} \quad (3.7)$$

$$\begin{aligned} \frac{S}{N_t k_B} &= \ln W \\ &= -\rho_1 \ln(\rho_1) - (1 - \rho_1) \ln(1 - \rho_1) \\ &\quad + \rho_1 \ln(v_d), \end{aligned} \quad (3.8)$$

where v_d is the number of configurations that the two monopoles in the pair can take, given say that the centre of mass of the pair is fixed. For a nearest-neighbour pair, $v_1 = 2$. For large values of d , we expect v_d to scale as $2 \times 4\pi d^2$. In practice, we shall approximate

$$v_d = v_1 \frac{8\pi d^2}{8\pi(d=1)^2} = v_1 d^2 = 2d^2. \quad (3.9)$$

Combining these results, we obtain the free energies (per tetrahedron) for free and bound pairs,

$$\begin{aligned} f_0 &= \frac{F_{\text{el}}}{N_t k_B} + \Delta \rho_0 \\ &\quad + T [\rho_0 \ln(\rho_0/2) + (1 - \rho_0) \ln(1 - \rho_0)] \end{aligned} \quad (3.10)$$

$$\begin{aligned} f_d &= (2\Delta - E_d)\rho_d \\ &\quad + T [\rho_d \ln(\rho_d) + (1 - \rho_d) \ln(1 - \rho_d)] \\ &\quad - T \rho_d \ln(v_d), \end{aligned} \quad (3.11)$$

as a function of the densities ρ_0 and ρ_d , $d = 1, \dots, \ell_B$. The equilibrium free energy of the entire system is then obtained minimizing the sum

$$f_{\text{tot}} = f_0 + f_1 + \dots + f_{\ell_B}$$

with respect to $\rho_0, \rho_1, \dots, \rho_{\ell_B}$.

Unlike ρ_0 , already considered in Sec. II B, the ρ_d are obtained straightforwardly as

$$\rho_d = \frac{v_d e^{-(2\Delta - E_d)/T}}{1 + v_d e^{-(2\Delta - E_d)/T}}. \quad (3.12)$$

Clearly, an intrinsic limit of validity of the theory is given by the condition that

$$\rho_{\text{tot}} \equiv \rho_0 + 2 \sum_{d=1}^{\ell_B} \rho_d \leq 1. \quad (3.13)$$

In addition, we are of course in particular interested in $\rho_0 \gg 2 \sum_{d=1}^{\ell_B} \rho_d = \rho_b$.

The behaviour of ρ_0 , ρ_1 , ρ_b and ρ_{tot} as a function of temperature in the regime of interest to spin ice is shown in Fig. 5. While at $T = 1$ K the bound pairs make up for approximately

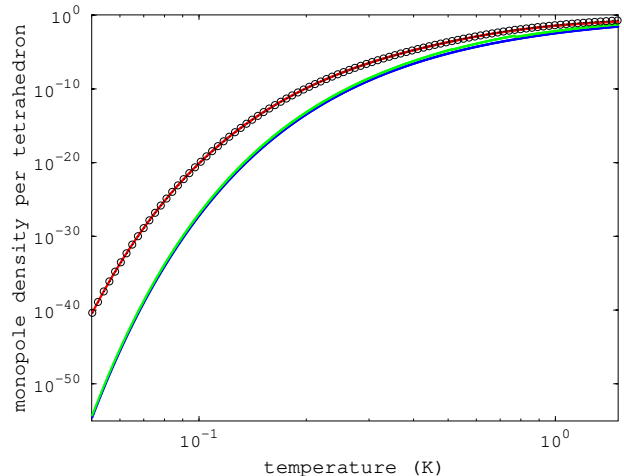


FIG. 5. Behaviour of ρ_0 (red), ρ_1 (blue), ρ_b (green), and ρ_{tot} (open black circles). In the regime of interest to spin ice physics, the total monopole density is dominated, at equilibrium, by the free monopoles.

16% of the monopoles in the system, this quickly drops to 7% at $T = 500$ mK and to $\lesssim 10^{-5}\%$ for $T \lesssim 100$ mK.

Of course, all the considerations in this section apply when the system is in thermal equilibrium. This is known not to be always the case in experimental settings involving spin ice materials! For example, as discussed in Ref. 23, fast variations in the temperature of a sample can lead to a “population inversion”, whereby a relatively high density of monopoles survives *out of equilibrium* down to very low temperatures, mostly forming nearest-neighbouring pairs ($\rho_{\text{tot}} \simeq \rho_1$)²³.

The arguments presented in this section are akin to the so-called Bjerrum correction to DH. The latter typically leads, at low temperatures, to the condensation of all monopoles into bound pairs. This is an artifact due to the neglecting of monopole-pair interactions, as discussed in Ref. 31.

Our results do not exhibit any such condensation. The reason for this difference in behaviour are to be found in the large monopole cost with respect to the Coulomb energy at nearest-neighbour distance. The net energy gain in the formation a bound pair is insufficient to compensate for the corresponding entropy loss. The situation would be dramatically different if the creation cost of the monopoles were lowered such that it can be offset by the Coulomb attraction to another monopole.

For completeness, we mention that for sufficiently large Coulomb attraction the chemical potential of a bound pair would have the *opposite sign* with respect to that of a free monopole, leading to a collapse of the system into an ionic crystal of monopoles. In spin language, this translates into an instability of spin ice to an ordered ground state.

IV. COMPARISON OF DH WITH MONTE CARLO

We compare the DH results above with Monte Carlo (MC) simulations using the spin ice parameters in Ref. 29, reported in the previous section. The Ewald summation technique was used for the long range dipolar interactions between the spins¹. We used systems of size $16L^3 = 3456$ spins ($L = 6$) and single spin flip updates.

A. Monopole density

A first comparison between the non-interacting limit and the DH approach can be done by looking at the resulting monopole density as a function of temperature, Eq. (2.5) and the numerical solution to (2.13), illustrated in Fig. 6 together with the monopole density from Monte Carlo simulations of dipolar spin ice.

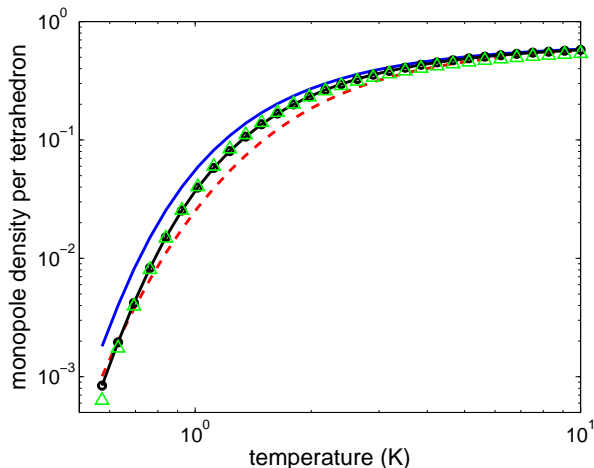


FIG. 6. Monopole density from numerical simulations (green triangles), compared to the analytical result in the non-interacting approximation (dashed red line) and in the DH approximation (solid blue line). Note that there are no fitting parameters. An improved agreement between the simulations and the DH approximation obtains if we adjust the bare monopole cost to $\Delta_{MC} = 4.7$ K (black dotted curve).

The agreement between DH and MC results is already quite reasonable yet it improves considerably if we tune the bare monopole cost to $\Delta_{MC} = 4.7$ K. As mentioned above, we believe the origin of this adjustment to be in the short-distance physics beyond the dumbbell model of Ref. 12. In quantities

sensitive to such short range details, such as Δ , this 8% discrepancy is not unreasonable.

B. Heat capacity

Given the DH free energy (expressed in units of degree Kelvin per Dy ion), one can obtain the heat capacity of the system in units of $\text{J mol}^{-1}\text{K}^{-1}$ via the thermodynamic relation

$$c_V = -N_A k_B T \partial_T^2 (F/N_s k_B), \quad (4.1)$$

where N_A is Avogadro's number, $\beta = 1/k_B T$, and k_B is the Boltzmann constant.

In MC simulations, c_V can be obtained by the usual fluctuation-dissipation route, measuring the average energy $\langle \varepsilon \rangle$ and its fluctuations,

$$c_V = \frac{RN_s}{T^2} [\langle \varepsilon^2 \rangle - \langle \varepsilon \rangle^2]. \quad (4.2)$$

A comparison between the non-interacting calculations, Eq. (2.5) and Eq. (2.4), the DH calculations, Eq. (2.13) and Eq. (2.12), the single tetrahedron approximation in Appendix A, and Monte Carlo simulations is shown in Fig. 7.

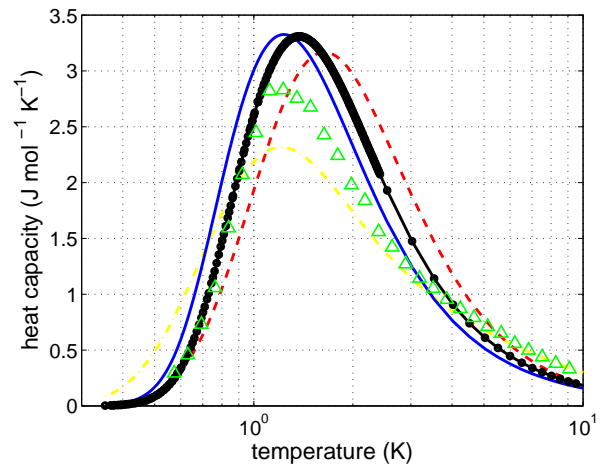


FIG. 7. Heat capacity from numerical simulations (green triangles), compared to the analytical result in the non-interacting approximation (dashed red line) and in the DH approximation (solid blue line). Note that there are no fitting parameters. Like for the density (cf. Fig. 6), improved agreement between the simulations and the DH solution is obtained for a bare monopole cost $\Delta_{MC} = 4.7$ K (black dotted curve). The single-tetrahedron approximation discussed in Appendix A can only be made to agree with the experimental results on a very narrow temperature range, even if we use J_{eff} as a fitting parameter (dash-dotted yellow line).

Consistently with the monopole density results, a comparison of the heat capacity from DH theory and simulations also shows improved agreement using $\Delta_{MC} = 4.7$ K instead of

$\Delta = 4.35$ K. We shall see in Sec. VI that an 8% larger value of Δ with respect to Eq. (3.1) is also consistent with the comparison between DH theory and experimental results.

The results in Fig. 6 and in Fig. 7 clearly show that: (i) a theory of point-like Coulomb-interacting charges (in particular with the improved value of the bare monopole cost) goes a long way into capturing the physics of spin ice, much better than conventional approaches based on truncated cluster expansions of the free energy of the system; (ii) the long-range nature of the interactions is necessary for understanding the low-temperature properties of spin ice materials.

V. ENTROPIC CHARGE: ROLE OF THE UNDERLYING SPINS

In disregarding the underlying spins in the Debye-Hückel approximation to the free energy of spin ice, we fail to account for quadrupolar corrections to the monopole description¹² (of which we have seen an effect in the value of the bare monopole cost Δ). We also neglect additional spin entropic contributions (other than the entropy of mixing of the monopoles)⁴⁻⁸.

The latter take the form of an entropic charge that adds onto the real magnetic charge (or, rather, magnetic and entropic coupling constants add) for the monopole Coulomb interactions. In Appendix B we derive an analytical expression for the entropic interaction strength and confirm the result by comparing it to Monte Carlo simulations. One can then repeat the DH calculations including the entropic correction. The results are shown in Fig. 8 (dashed cyan lines), in comparison to the previous results (solid blue lines), for the parameters in Sec. IV with $\Delta_{MC} = 4.7$ K. The behaviour of the monopole

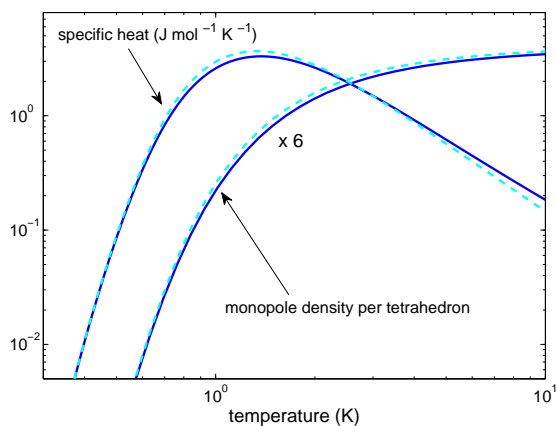


FIG. 8. Effects of the entropic charge (dashed cyan lines) on the Debye-Hückel estimate of the heat capacity and monopole density (solid blue lines).

density and of the heat capacity clearly show that the entropic contribution can be safely neglected in the low temperature regime where the DH approximation is valid. It is worth noting that the relative strength of magnetic and entropic charges

can in principle be tuned straightforwardly, e.g. by decreasing D at fixed J_{eff} , as the magnetic monopole charge is proportional to D , whereas the scale determining the applicability of the monopole picture is set by J_{eff} .

Indeed, for the nearest-neighbour model with $D = 0$, where there is no magnetic monopole charge, one would be considering a Coulomb gas with entropic interactions only. Debye screening in such a setting has already been considered in two dimensions, for the entropic Coulomb gas encountered in the square lattice monomer-dimer model.²⁸

VI. EXPERIMENT

We now proceed to compare the DH results with experimental data on $\text{Dy}_2\text{Ti}_2\text{O}_7$. We find good agreement, which is further improved if we use the latest material parameters from Ref. 26 instead of those in Ref. 29. Namely, the magnetic moment of the rare earth ions is $9.87 \mu_B$ instead of $10 \mu_B$; the diamond lattice constant is 4.38 \AA instead of 4.34 \AA ; and the nearest-neighbour exchange coupling varies between -3.53 and -3.26 , instead of $J = -3.72$ K.

These values result in a new magnetic monopole charge of $4.5 \mu_B/\text{\AA}$; a nearest-neighbour interaction strength between monopoles $E_{\text{nn}} = 2.88$ K instead of 3.06 K; a dipolar coupling constant $D = 1.32$ K instead of 1.41 K; and a bare monopole cost in the range $(4.05, 4.23)$ K instead of $\Delta = 4.35$ K. We reiterate that there are also small corrections due to further-range superexchange and the quadrupolar interactions, which are not easily incorporated into the DH framework.

A. Heat capacity

A comparison between the experimentally measured heat capacity and the one obtained from DH theory, shows again that the bare monopole cost $\Delta \in (4.05, 4.23)$ K from Eq. (3.1) is somewhat too small. Better agreement can be obtained if, as in the comparison with MC simulations, we allow for an 8% increase in the value of $\Delta \in (4.37, 4.57)$ K (see Fig. 9). This is in agreement with the results presented in Ref. 10 (Fig. 1), where a value of $\Delta = 4.35$ K¹² was used.

B. ‘Dressed’ monopole energy and AC susceptibility

The bare monopole cost Δ is half the energy required for creating and separating to infinity a pair of monopoles against their long-range Coulomb attraction. When other monopoles are present, screening effectively truncates the range of the interactions and there is no further energy cost to separating a pair beyond the screening length. In this case it is more appropriate to consider the ‘dressed’ monopole energy Δ_d as the energy per monopole that it takes to create a pair and separate it beyond the screening length. It is indeed the energy Δ_d – rather than Δ – that controls for instance the equilib-

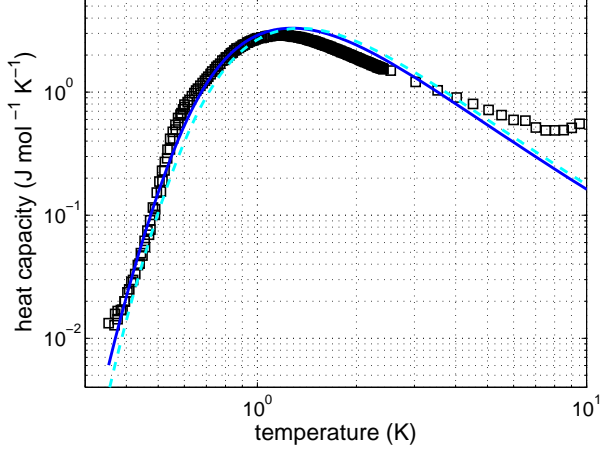


FIG. 9. Experimental results for the heat capacity of $\text{Dy}_2\text{Ti}_2\text{O}_7$ (black squares) from Ref. 10, in units of J/mol K , compared to the analytical result from Debye-Hückel theory with $\Delta = 4.37 \text{ K}$ (solid blue line) and $\Delta = 4.57 \text{ K}$ (dashed cyan line).

rium density of the monopoles $\rho \sim e^{-\Delta_d/T}$ at intermediate temperatures.

Given the creation energy for a nearest neighbour pair $\Delta_s = 2\Delta - E_{\text{nn}}$ and the expression for the DH screening length, Eq. (3.5), one obtains

$$\begin{aligned} 2\Delta_d(T) &= 2\Delta - E_{\text{nn}} + \left(E_{\text{nn}} - \frac{\mu_0}{4\pi k_B} \frac{q^2}{\xi_{\text{Debye}}(T)} \right) \\ &= 2\Delta - E_{\text{nn}} \frac{a_d}{\xi_{\text{Debye}}(T)}, \end{aligned} \quad (6.1)$$

whose behaviour is illustrated in the inset of Fig. 10.

A place where this screening effect of the magnetic monopoles becomes particularly evident is in susceptibility measurements of magnetic relaxation time scales^{19,21}. Given that the monopoles are responsible for any changes in magnetisation in a spin ice configuration, the ability of the system to respond to an applied magnetic field is affected by the monopole density. For non-interacting monopoles, Ryzhkin showed that in the low temperature, hydrodynamic regime the characteristic susceptibility time scale τ is inversely proportional to the monopole density²⁰,

$$\tau^{-1} \propto \nu T \rho(T), \quad (6.2)$$

where ν is the mobility of the monopoles. This result is likely to be asymptotically correct as $T \rightarrow 0$ at zero wavevector even in presence of Coulomb interactions, although it is modified at finite wavevectors.

In App. C, we show that $\nu \sim 1/T$ under the assumption that Metropolis dynamics are a good approximation to the microscopic spin flip processes in spin ice. Therefore,

$$\tau \propto 1/\rho(T). \quad (6.3)$$

As we argued above, at intermediate temperatures $\rho(T)$ is controlled by the dressed monopole energy $\Delta_d(T)$ rather than

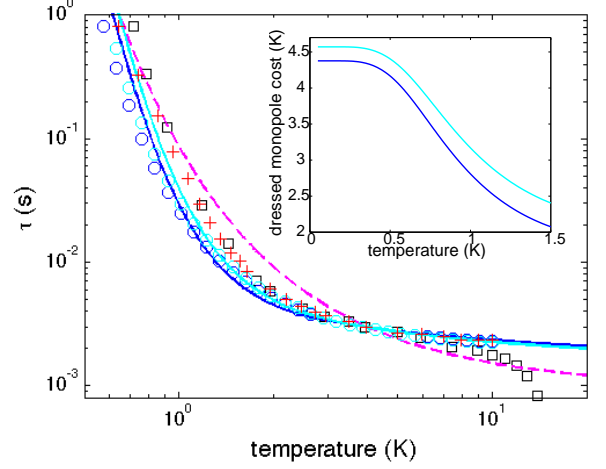


FIG. 10. Experimental magnetic relaxation time scale τ as a function of temperature from susceptibility data, Ref. 19 (black open squares). The rapid increase in τ at low temperatures is due to the paucity of defects responsible for the magnetic rearrangement of a spin ice configuration (namely, the monopoles). This increase cannot be described by a single exponential (activated behaviour), as it is evident for instance by comparison with the curve $\tau = \tau_0 \exp(\Delta/T)$ (dashed magenta line), say with $\Delta = 4.5 \text{ K}$. On the contrary, a much better agreement is obtained if we replace the bare monopole energy Δ with the ‘dressed’ energy $\Delta_d(T)$ (solid blue curve for $\Delta = 4.37 \text{ K}$ and solid cyan curve for $\Delta = 4.57 \text{ K}$). This is compared to $\tau \propto 1/\rho$, where ρ is obtained from the DH approximation (blue open circles for $\Delta = 4.37 \text{ K}$ and cyan open circles for $\Delta = 4.57 \text{ K}$), showing that indeed the dressing of Δ accounts for the leading non-exponential correction in the temperature dependence in the monopole density. The microscopic time scale was set by imposing that the analytical results pass through the experimental data point at 4 K (see Ref. 21). The inset shows the ‘dressed’ monopole energy Δ_d as a function of temperature (solid blue curve for $\Delta = 4.37 \text{ K}$ and solid cyan curve for $\Delta = 4.57 \text{ K}$).

the bare energy Δ . Indeed, τ is poorly fitted by a single exponential^{19,21} such as $\tau = \tau_0 \exp(\Delta/T)$. On the contrary, the curve $\tau = \tau_0 \exp[\Delta_d(T)/T]$, captures correctly the faster-than-exponential growth of τ at low temperatures, despite the fact that it still significantly underestimates the experimental value of τ (see Fig. 10).³⁰

Given the good agreement between DH theory and experiments regarding the heat capacity of the system (Fig. 9) and given that a similarly good agreement in the heat capacity from Monte Carlo simulations implied a good agreement also for the monopole density (Fig. 6 and Fig. 7), one would expect that $\rho(T)$ from Debye-Hückel used in Fig. 10 is in fact a good estimate of the experimental monopole density. Therefore, the fact that Eq. (6.3) underestimates the experimental results even when using $\rho(T)$ from DH theory is likely due to corrections to the dependence $\tau \propto 1/\rho(T)$ arising from Coulomb interactions at intermediate monopole densities.

At the lowest temperatures (provided of course no ordering or freezing intervenes, as it likely would), when monopole separation and screening length both diverge, the effective

$\Delta_d \rightarrow \Delta$, and hence we expect the superexponential behaviour to go away and the curve to follow the standard Arrhenius behaviour $\tau \sim \exp(\Delta/T)$.

From a purely phenomenological perspective, it is interesting to notice that a very good agreement between DH theory and experiments on the susceptibility time scale τ (at intermediate temperatures) can be obtained by substituting Eq. (6.3) with $\tau \propto 1/\rho^\eta(T)$, with $\eta = 3/2$ for $\Delta = 4.37$ K and $\eta = 4/3$ for $\Delta = 4.57$ K (see Fig. 11). Further work is

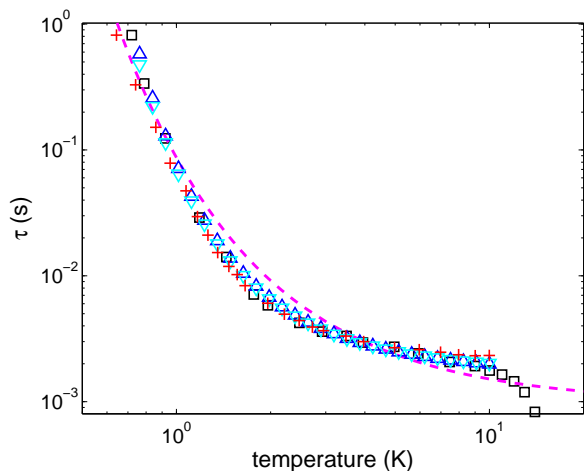


FIG. 11. Experimental magnetic relaxation time scale τ as a function of temperature from susceptibility data, Ref. 19 (black open squares). The temperature dependence is captured very accurately by a phenomenological equation of the type $\tau \propto 1/\rho^\eta$, where ρ is obtained from the DH approximation (blue upward triangles for $\Delta = 4.37$ K and $\eta = 3/2$; cyan downward triangles for $\Delta = 4.57$ K and $\eta = 4/3$). The dashed magenta line illustrates the curve $\tau = \tau_0 \exp(\Delta/T)$ with $\Delta = 4.5$ K, for comparison.

needed to understand the reasons behind such a good overlap.

VII. BEYOND DEBYE-HÜCKEL

Debye-Hückel theory is probably the simplest approximation to obtain the free energy of a gas of Coulomb interacting particles short of ignoring interactions altogether. A number of improvements are available in the vast literature on the subject³¹, which one can use to obtain a more accurate description of the magnetic monopole behaviour in spin ice.

Without actually implementing them, we briefly recall hereafter two common extensions of the DH model. Firstly, Debye-Hückel theory neglects the association of monopoles into neutral dipolar pairs, which we have already briefly discussed above (see Ref. 31 and references therein). Following Bjerrum³² (Bj) one can account for such bound pairs, thus compensating in good part for the uncontrolled linearisation of the Poisson-Boltzmann equation that is at the basis of the DH self-consistent solution. However, whilst being an overall refinement of DH, DHBj theory leads to unrealistic features

in the phase diagram of the system³¹, with an exponential increase in the low-temperature fraction of neutral pairs draining the free monopole density to zero. This can (and ought to) be compensated by a further extension to include interactions between dipolar bound pairs and free monopoles, leading to the so called dipole-ionic (DI) contribution³¹. The full DHBjDI theory indeed cures the unphysical features identified for DHBj, while remaining of course only an approximation to the exact free energy of the system.

Further improvements on the DHBjDI theory include accounting for hard-core (HC) effects³¹. It is certainly worthwhile developing the theory further in this direction, especially in settings or for quantities where new phenomena (e.g., a dominant population of bound pairs), rather than only quantitative corrections, ensue.

VIII. CONCLUSIONS

In summary, we have presented a theory for the low-temperature physics of spin ice within the Debye-Hückel framework familiar from the study of (electric) Coulomb liquids. The success of this simple approach in treating the low-energy physics of spin ice is a testament to the power of the ‘variable transformation’ from magnetic dipoles to magnetic monopoles appropriate to the Coulomb phase with its emergent gauge field.

With this first step accomplished, next on the wishlist are a number of items some of which should push our attention beyond the framework provided by the DH paradigm. Firstly, a more detailed understanding of spin ice (hydro)dynamics; secondly, an extension of this theory to a broader class of parent Hamiltonians, perhaps even including coherent quantum dynamics; and thirdly, contact with all the non-equilibrium experiments suggesting that not only the sparseness of monopoles but also phononic physics plays a role in the freezing of spin ice around T_f .³³

ACKNOWLEDGMENTS

We are very grateful to our experimental collaborators of Ref. 10 – in particular Santiago Grigera, Klaus Kiefer, Bastian Klemke, Michael Meissner, Jonathan Morris, Kirilly Rule, Damian Slobinsky and Alan Tennant – for the discussions and experimental measurements which motivated us to pursue the Coulomb gas analogy in detail as reported here.

This work was supported in part by EPSRC Postdoctoral Research Fellowship EP/G049394/1 (C.C.) and by NSF Grant Number DMR-1006608 (S.L.S.). We mutually acknowledge hospitality and travel support for visits to our respective institutions.

Appendix A: Single tetrahedron approximation

An alternative approximation that can be used to obtain the spin ice free energy and related thermodynamic quantities is to

use a truncated cluster expansion. Most simply, this amounts to computing explicitly the free energy of an isolated tetrahedron by direct summation over all 2^4 states.

At this level, all interactions are nearest-neighbour ones. In terms of this effective short range coupling J_{eff} , the partition function of a tetrahedron is

$$Z = \left[6 + 8e^{-2J_{\text{eff}}/T} + 2e^{-8J_{\text{eff}}/T} \right]^{N_t}. \quad (\text{A1})$$

From this, one can estimate the partition function of the entire system,

$$Z = 2^{N_s} \left[\frac{6 + 8e^{-2J_{\text{eff}}/T} + 2e^{-8J_{\text{eff}}/T}}{16} \right]^{N_s/2}, \quad (\text{A2})$$

and thus the free energy per spin in degrees Kelvin, $F/N_s k_B = -(T/N_s) \ln Z$.

Substituting into Eq. (4.1), we obtain the heat capacity of the system (in units of J/K per Dy ion),

$$c_V = \frac{24k_B J_{\text{eff}}^2}{T^2} \frac{e^{6J_{\text{eff}}/T} (3 - 2e^{2J_{\text{eff}}/T} + e^{4J_{\text{eff}}/T})}{(1 - e^{2J_{\text{eff}}/T} + e^{4J_{\text{eff}}/T} + 3e^{6J_{\text{eff}}/T})^2}. \quad (\text{A3})$$

The choice of $J_{\text{eff}} = 5D/3 + J/3 = 1.11$ K, which corresponds to the nearest-neighbour interaction strength from the exchange plus dipolar coupling constants, yields a very poor agreement with the experimental data (not shown). The situation improves slightly if we take advantage of the projective equivalence between dipolar and nearest-neighbour interactions on the pyrochlore lattice³⁴. Instead of truncating the dipolar contribution to $5D/3$, one can therefore use the effective value of J_{nn} that yields the same low-energy spectrum as from the long range dipolar interactions. This value can be derived using the dumbbell decomposition in Ref. 12, $J_{\text{eff}} = 1.45$ K. The result is shown in Fig. 1 of Ref. 10 and it is indeed in quantitative agreement with the experimental data at high temperatures $T \gtrsim 2$ K, as expected of a cluster expansion of the free energy.

Note that even if we allow J_{eff} to vary as a fitting parameter in the theory, the shape of $c_V(T)$ does not change significantly and it can be brought to agree with the experimental data only over a very narrow temperature interval. By comparison, this highlights even more how effective the Debye-Hückel free energy is at capturing the low energy fluctuations in dipolar spin ice.

Appendix B: Entropic monopole charge

The effective description of spin-ice in the absence of monopoles is given by the probability distribution of a magnetostatic-like (divergenceless) field²²

$$\mathcal{P} \propto \exp \left[-\frac{\mathcal{K}}{2} v_{\text{cell}}^{-1} \int \left| \vec{B}^{\text{ent}}(r) \right|^2 d^3 r \right] \quad (\text{B1})$$

$$\times \exp \left[-\frac{\mu_0}{2k_B T} \int \left| \vec{H}^{\text{mag}}(r) \right|^2 d^3 r \right]. \quad (\text{B2})$$

The first term Eq. (B1) is purely entropic in origin. The geometric field $\vec{B}^{\text{ent}}(r)$ is obtained from coarse graining fixed-length vectors that identify the local direction of the spins in the system. Here v_{cell} is the volume of the primitive unit cell (Fig. 12). Introducing the coarse grained (dimensionless) field $\vec{B}(r)$ defined at the centre of each tetrahedron (belonging to one of the two sublattices) as

$$\begin{pmatrix} B_x \\ B_y \\ B_z \end{pmatrix} = \frac{1}{\sqrt{3}} \begin{pmatrix} 1 & 1 & -1 & -1 \\ 1 & -1 & 1 & -1 \\ 1 & -1 & -1 & 1 \end{pmatrix} \begin{pmatrix} S_0 \\ S_1 \\ S_2 \\ S_3 \end{pmatrix} \quad (\text{B3})$$

the stiffness coefficient can be determined to be $\mathcal{K} = 3/8$. (Note that we used a different field normalisation with respect to Ref. 35, so as to preserve the underlying spin length equal to 1.)

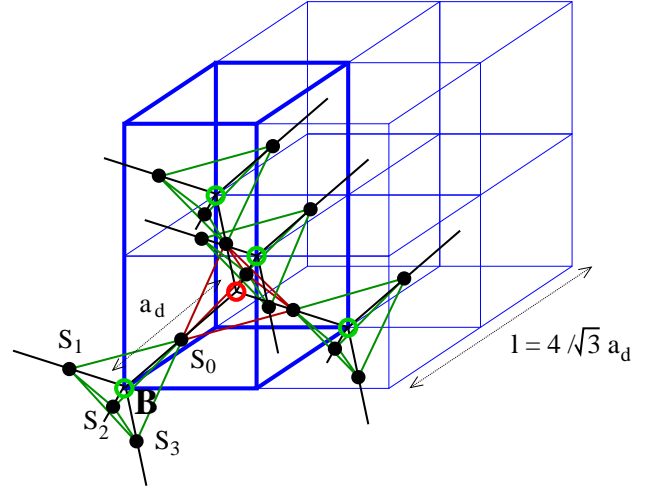


FIG. 12. Lattice conventions. The highlighted portion of the blue cube (i.e., the 16-spin cubic unit cell in spin ice) corresponds to a possible choice of the primitive unit cell in the fcc lattice formed by the centres of one sublattice of tetrahedra in the pyrochlore lattice (circled in green in the figure).

The second term Eq. (B2) accounts for the magnetic energy stored in a spin ice configuration (devoid of monopoles). In this case, $\vec{H}^{\text{mag}}(r)$ is the magnetic field generated by the spin magnetic moments μ pointing in the local spin direction (μ_0 is the permeability of the vacuum, k_B is the Boltzmann constant and T is the temperature of the system).

Given that the total field $\vec{B} = \mu_0(H + M)$ is always divergenceless, the field $\vec{H}^{\text{mag}}(r)$ can be equivalently replaced by the magnetisation per unit volume M , which in turn can be obtained by coarse graining the spin magnetic moments. Using the scheme (B3) already adopted for $\vec{B}^{\text{ent}}(r)$ over a primitive unit cell, we have that

$$\left| \vec{H}^{\text{mag}}(r) \right| = \left| \vec{M}(r) \right| = \frac{\mu}{v_{\text{cell}}} \left| \vec{B}^{\text{ent}}(r) \right|. \quad (\text{B4})$$

Therefore, the difference between the two terms Eq. (B1) and

Eq. (B2) can be reduced to different coefficients

$$\frac{\mathcal{K}}{v_{\text{cell}}} \quad \text{vs} \quad \frac{\mu_0 \mu^2}{k_B T v_{\text{cell}}^2} \quad (\text{B5})$$

to the same integral $\int |\vec{B}^{\text{ent}}(r)|^2 d^3 r$.

It is convenient to re-express the magnetic coefficient in terms of the magnetic Coulomb energy of two monopoles placed in adjacent tetrahedra (expressed in degrees Kelvin),

$$E_{\text{nn}} = \frac{\mu_0}{4\pi k_B} \frac{q^2}{a_d} = \frac{\mu_0}{\pi k_B} \frac{\mu^2}{a_d^3} \quad (\text{B6})$$

$$\Rightarrow \frac{\mu_0 \mu^2}{k_B T v_{\text{cell}}^2} = \frac{E_{\text{nn}}}{T} \frac{\pi a_d^3}{v_{\text{cell}}^2}, \quad (\text{B7})$$

where we used the fact that $q = 2\mu/a_d$, a_d being the diamond lattice constant. By comparison with the entropic coefficient, we can then identify the entropic counterpart to the nearest-neighbour Coulomb energy,

$$\frac{E_{\text{nn}}^{\text{ent}}}{T} \frac{\pi a_d^3}{v_{\text{cell}}^2} = \frac{\mathcal{K}}{v_{\text{cell}}} \quad (\text{B8})$$

$$\Rightarrow \frac{E_{\text{nn}}^{\text{ent}}}{T} = \frac{\mathcal{K}}{\pi} \frac{v_{\text{cell}}}{a_d^3}. \quad (\text{B9})$$

If we finally use the fact that v_{cell} is 1/4 of the volume of the 16-spin cubic unit cell in spin ice, $v = (4a_d/\sqrt{3})^3$, and that with the coarse graining (B3) $\mathcal{K} = 3/8$, we arrive at the result

$$\frac{E_{\text{nn}}^{\text{ent}}}{T} = \frac{\mathcal{K}}{\pi} \frac{16}{3\sqrt{3}} = \frac{2}{\sqrt{3}\pi} \simeq 0.36755. \quad (\text{B10})$$

It is interesting to convert this value into an entropic monopole charge :

$$\begin{aligned} q_{\text{ent}} &= \sqrt{\frac{4\pi a_d k_B E_{\text{nn}}^{\text{ent}}}{\mu_0}} = 1.48 \cdot 10^{-13} \sqrt{T} \\ &= 1.6 \sqrt{T} \mu_B / \text{\AA}. \end{aligned} \quad (\text{B11})$$

The entropic charge of a monopole becomes larger than the real magnetic charge only for $T \gtrsim 8$ K, well beyond the limit of validity of the monopole description of spin ice. In the experimentally relevant temperature range 0.1–1 K, the entropic contribution ranges from 1% to 10% of the real magnetic contribution to the energy of the monopoles.

In order to confirm this analytical estimate of the entropic Coulomb interaction strength in spin ice, we have run Monte Carlo simulations of the nearest-neighbour spin ice model, sampling only configurations with two monopoles (one positive, one negative). Such configurations are all isoenergetic and the monopole positions can be updated at every Monte Carlo step without rejection. Ergodicity was tested by computing spin-spin autocorrelation functions. The distribution of separation distances between the two monopoles was then sampled both in Monte Carlo time and across different initial configurations and random number seeds.

From Eq. B1, it follows that the entropic interaction between the two monopoles leads to a probability distribution

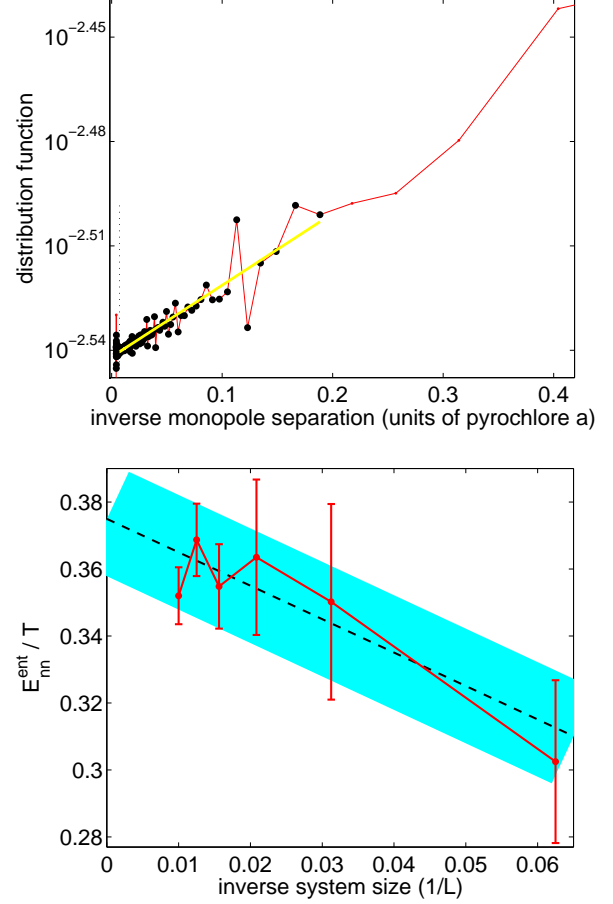


FIG. 13. Top Panel: Distribution of distances per lattice site between two monopoles in a spin ice configuration of $16 \times L^3$ spins, $L = 64$. (top panel, red curve). The expected form due to the entropic Coulombic interaction is $\mathcal{P} \sim \exp(E_{\text{nn}}^{\text{ent}}/TR)$ and the solid yellow line is the linear fit of $\ln P(R)$ as a function of $1/R$. Bottom Panel: Finite size scaling of the nearest neighbour entropic interaction $E_{\text{nn}}^{\text{ent}}/T$ vs. the inverse system size $1/L$, $L = 16, 32, 48, 64, 80, 100$. The dashed black line and shaded cyan region are a guide to the eye for a reasonable $L \rightarrow \infty$ extrapolation and confidence interval, leading to $E_{\text{nn}}^{\text{ent}}/T \simeq 0.375 \pm 0.015$.

of the form $\mathcal{P}(R) \sim R^2 \exp(E_{\text{nn}}^{\text{ent}}/TR)$, where R is the separation distance in units of the diamond lattice spacing. In particular, if we sample the distribution *per lattice site* at distance R , it has a purely exponential form $\sim \exp(E_{\text{nn}}^{\text{ent}}/TR)$, and one can obtain the value of $E_{\text{nn}}^{\text{ent}}/T$ from linear fits in semi-logarithmic scale (Fig. 13, top panel).

We repeated these fits for different system sizes in order to account for finite size scaling (illustrated in Fig. 13, bottom panel). Even though the accuracy of our simulations does not allow for a reliable extrapolation in the $L \rightarrow \infty$ limit, the nearest-neighbour entropic interaction strength appears to lie in the interval $E_{\text{nn}}^{\text{ent}}/T \simeq 0.375 \pm 0.015$, in reasonable agreement with the analytical value in Eq. (B10), $2/\sqrt{3}\pi \simeq 0.36755$.

Appendix C: Monopole mobility

The mobility of the monopoles in spin ice (and thus its temperature dependence) can be estimated from microscopic considerations, under the assumption that Metropolis-like equations govern the dynamics of the system^{23,36}.

The mobility of a particle is given by the ratio of its drift velocity v_d over the driving force strength qE , $\nu = v_d/(qE)$.

Under Metropolis dynamics for a particle with charge q in a field E , the average displacement in a single step is

$$\Delta x = \ell \frac{1 - e^{-\beta qV}}{1 + e^{-\beta qV}}, \quad (\text{C1})$$

where ℓ is the characteristic microscopic length scale, V is the potential difference for a single hopping process, 1 is the probability to hop in the direction of the field, and $\exp(-\beta qV)$ is the probability to hop in the opposite direction.

Note that, on a lattice, there can be several inequivalent forward and backward hoppings, depending on the direction of the field. For example, while a 45° field applied to charged particles living on a square lattice is described straightforwardly by the above equation (with $\ell = a/\sqrt{2}$, a being the lattice spacing), a 90° field on the same lattice allows for a forward, a backward, and two perpendicular hopping processes (see Fig. 14). One therefore needs to average over all of them

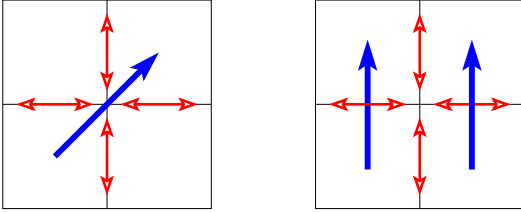


FIG. 14. Two examples of how the available hopping processes depend on the direction of the applied field on a square lattice: a 45° field (left) and a 90° field (right).

to obtain the correct value of Δx .

For convenience, we choose to define the mobility ν as

$$\frac{\Delta x/a}{\tau_0} = \frac{\ell}{a\tau_0} \frac{1 - e^{-\beta qV}}{1 + e^{-\beta qV}} \quad (\text{C2})$$

$$\equiv \nu qEa, \quad (\text{C3})$$

for small values of the applied field E . Here a is the (dimensionful) lattice constant and τ_0 is the microscopic time scale for a single MC step. At large temperatures with respect to the field strength, one can expand the exponentials and arrive at the expression

$$\nu = \frac{1}{\tau_0} \frac{1}{qEa} \frac{\ell}{a} \frac{1 - e^{-\beta qV}}{1 + e^{-\beta qV}} \quad (\text{C4})$$

$$= \frac{1}{\tau_0} \frac{\ell}{a} \frac{V/(Ea)}{2k_B T} + \mathcal{O}\left[\frac{(\beta V)^2}{qEa}\right]. \quad (\text{C5})$$

For example, the case of a generic field direction on the anisotropic square lattice, with lattice constants a and b , gives

$$\begin{aligned} \nu &= \frac{1}{\tau_0} \frac{1}{qEa^2} \frac{a \cos \theta + b \sin \theta - a \cos \theta e^{-\beta qEa \cos \theta} - b \sin \theta e^{-\beta qEb \sin \theta}}{1 + 1 + e^{-\beta qEa \cos \theta} + e^{-\beta qEb \sin \theta}} \\ &\simeq \frac{1}{\tau_0} \frac{1}{4k_B T} \frac{a^2 \cos^2 \theta + b^2 \sin^2 \theta}{a^2} + \mathcal{O}(\beta^2 E). \end{aligned} \quad (\text{C6})$$

If the lattice is isotropic ($a = b$) the mobility is independent of the direction of the applied field,

$$\nu \simeq \frac{1}{\tau_0} \frac{1}{4k_B T} + \mathcal{O}(\beta^2 E). \quad (\text{C7})$$

The mobility of monopoles on an isotropic diamond lattice,

of lattice constant a_d , with respect to a generic field direction \hat{e} can be computed in a similar way, with the additional care that there are now two inequivalent sublattices. With respect to one sublattice, we obtain

$$\begin{aligned}
\nu &= \frac{1}{\tau_0} \frac{1}{qEa_d} \frac{1}{\sqrt{3}} \frac{(\hat{e}_1 + \hat{e}_2 + \hat{e}_3) \min \left[1, e^{\beta q E a_d (\hat{e}_1 + \hat{e}_2 + \hat{e}_3) / \sqrt{3}} \right] + (\hat{e}_1 - \hat{e}_2 - \hat{e}_3) \min \left[1, e^{\beta q E a_d (\hat{e}_1 - \hat{e}_2 - \hat{e}_3) / \sqrt{3}} \right]}{\min \left[1, e^{\beta q E a_d (\hat{e}_1 + \hat{e}_2 + \hat{e}_3) / \sqrt{3}} \right] + \min \left[1, e^{\beta q E a_d (\hat{e}_1 - \hat{e}_2 - \hat{e}_3) / \sqrt{3}} \right]} \\
&\quad + \frac{(-\hat{e}_1 + \hat{e}_2 - \hat{e}_3) \min \left[1, e^{\beta q E a_d (-\hat{e}_1 + \hat{e}_2 - \hat{e}_3) / \sqrt{3}} \right] + (-\hat{e}_1 - \hat{e}_2 + \hat{e}_3) \min \left[1, e^{\beta q E a_d (-\hat{e}_1 - \hat{e}_2 + \hat{e}_3) / \sqrt{3}} \right]}{\min \left[1, e^{\beta q E a_d (-\hat{e}_1 + \hat{e}_2 - \hat{e}_3) / \sqrt{3}} \right] + \min \left[1, e^{\beta q E a_d (-\hat{e}_1 - \hat{e}_2 + \hat{e}_3) / \sqrt{3}} \right]} \\
&\simeq \frac{1}{\tau_0} \frac{1}{12k_B T} \left[(\hat{e}_1 + \hat{e}_2 + \hat{e}_3)^2 \Theta_{<}(\hat{e}_1 + \hat{e}_2 + \hat{e}_3) + (\hat{e}_1 - \hat{e}_2 - \hat{e}_3)^2 \Theta_{<}(\hat{e}_1 - \hat{e}_2 - \hat{e}_3) \right. \\
&\quad \left. + (-\hat{e}_1 + \hat{e}_2 - \hat{e}_3)^2 \Theta_{<}(-\hat{e}_1 + \hat{e}_2 - \hat{e}_3) + (-\hat{e}_1 - \hat{e}_2 + \hat{e}_3)^2 \Theta_{<}(-\hat{e}_1 - \hat{e}_2 + \hat{e}_3) \right] + \mathcal{O}(\beta^2 E), \tag{C8}
\end{aligned}$$

where $\Theta_{<}(x) = \Theta(-x)$ is the Heaviside theta function. With respect to the other sublattice, we obtain

$$\begin{aligned}
\nu &\simeq \frac{1}{\tau_0} \frac{1}{12k_B T} \left[(\hat{e}_1 + \hat{e}_2 + \hat{e}_3)^2 [1 - \Theta_{<}(\hat{e}_1 + \hat{e}_2 + \hat{e}_3)] + (\hat{e}_1 - \hat{e}_2 - \hat{e}_3)^2 [1 - \Theta_{<}(\hat{e}_1 - \hat{e}_2 - \hat{e}_3)] \right. \\
&\quad \left. + (-\hat{e}_1 + \hat{e}_2 - \hat{e}_3)^2 [1 - \Theta_{<}(-\hat{e}_1 + \hat{e}_2 - \hat{e}_3)] + (-\hat{e}_1 - \hat{e}_2 + \hat{e}_3)^2 [1 - \Theta_{<}(-\hat{e}_1 - \hat{e}_2 + \hat{e}_3)] \right] + \mathcal{O}(\beta^2 E). \tag{C9}
\end{aligned}$$

If we finally take the average of both sublattices, we arrive at

$$\begin{aligned}
\nu &\simeq \frac{1}{2\tau_0} \frac{1}{12k_B T} \left[(\hat{e}_1 + \hat{e}_2 + \hat{e}_3)^2 + (\hat{e}_1 - \hat{e}_2 - \hat{e}_3)^2 \right. \\
&\quad \left. + (-\hat{e}_1 + \hat{e}_2 - \hat{e}_3)^2 + (-\hat{e}_1 - \hat{e}_2 + \hat{e}_3)^2 \right] \\
&\quad + \mathcal{O}(\beta^2 E) \\
&\simeq \frac{1}{6} \frac{1}{\tau_0} \frac{1}{k_B T} + \mathcal{O}(\beta^2 E), \tag{C10}
\end{aligned}$$

independently of the direction of the field E .

If the magnetic monopoles on the diamond lattice are in fact the collective excitations in a spin ice system, one needs to take into account the constraint that one of the three possible hopping directions is essentially forbidden, as it would create doubly charged excitations. Taking the average over the possible forbidden directions does not introduce a dependence

on the field direction and we can therefore choose to compute the mobility in a [100] magnetic field for convenience:

$$\begin{aligned}
\nu &= \frac{1}{2\tau_0} \frac{1}{qEa_d} \frac{1}{\sqrt{3}} \frac{2 - e^{-\beta q E (a_d / \sqrt{3})}}{2 + e^{-\beta q E (a_d / \sqrt{3})}} \\
&\quad + \frac{1}{2\tau_0} \frac{1}{qEa_d} \frac{1}{\sqrt{3}} \frac{1 - 2e^{-\beta q E (a_d / \sqrt{3})}}{1 + 2e^{-\beta q E (a_d / \sqrt{3})}} \\
&\simeq \frac{4}{27} \frac{1}{\tau_0} \frac{1}{k_B T}, \tag{C11}
\end{aligned}$$

Notice that these results are independent of whether the potential and field had an entropic or magnetic origin, provided that the assumption of the field being smooth over distances of the order of the lattice spacing a_d holds. This definition of the mobility shows in fact that it depends only on some microscopic time scale τ_0 and on the thermal energy per particle in the system.

-
- ¹ S. W. de Leeuw, J. W. Perram, and E. R. Smith, Proc. R. Soc. Lond. A **373**, 27 (1980); Proc. R. Soc. Lond. A **373**, 57 (1980).
² S. T. Bramwell and M. J. P. Gingras, Science **294**, 1495 (2001).
³ A. P. Ramirez, A. Hayashi, R. J. Cava, R. Siddharthan, and B. S. Shastry, Nature **399**, 333 (1999).
⁴ D. A. Huse, W. Krauth, R. Moessner, and S. L. Sondhi, Phys. Rev. Lett. **91**, 167004 (2003).
⁵ R. Moessner and S. L. Sondhi, Phys. Rev. B **68**, 184512 (2003).
⁶ S. V. Isakov, K. Gregor, R. Moessner, and S. L. Sondhi, Phys. Rev. Lett. **93**, 167204 (2004).
⁷ M. Hermele, M. P. A. Fisher, and L. Balents, Phys. Rev. B **69**, 064404 (2004).
⁸ C. L. Henley, Phys. Rev. B **71**, 014424 (2005).
⁹ T. Fennell, P. P. Deen, A. R. Wildes, K. Schmalzl, D. Prabhakaran, A. T. Boothroyd, R. J. Aldus, D. F. McMorrow, and S. T. Bramwell, Science **326**, 415 (2009).
¹⁰ D. J. P. Morris, D. A. Tennant, S. A. Grigera, B. Klemke,

- C. Castelnovo, R. Moessner, C. Czternasty, M. Meissner, K. C. Rule, J.-U. Hoffmann, K. Kiefer, S. Gerischer, D. Slobinsky, and R. S. Perry, Science **326**, 411 (2009).
¹¹ H. Kadowaki, N. Doi, Y. Aoki, Y. Tabata, T. J. Sato, J. W. Lynn, K. Matsuhira, and Z. Hiroi, J. Phys. Soc. Japan **78**, 103706 (2009).
¹² C. Castelnovo, R. Moessner, and S. L. Sondhi, Nature **451**, 42 (2008).
¹³ Note that the correlations have a dipolar piece at $T > 0$ also, due to the long ranged interactions.
¹⁴ S. T. Bramwell, S. R. Giblin, S. Calder, R. Aldus, D. Prabhakaran, and T. Fennell, Nature **461**, 956 (2009).
¹⁵ C. Castelnovo, Chem. Phys. Chem. **11**, 557 (2010).
¹⁶ S. R. Giblin, S. T. Bramwell, P. C. W. Holdsworth, D. Prabhakaran, and I. Terry, Nature Physics **7**, 252 (2011).
¹⁷ K. Matsuhira, Y. Hinatsi, K. Tenya, and T. Sakakibara, J. Phys.: Condens. Matter **12**, L649 (2000).
¹⁸ K. Matsuhira, Y. Hinatsu, and T. Sakakibara, J. Phys. Condens. Matter **13**, L737 (2001).

- ¹⁹ J. Snyder, B. G. Ueland, J. S. Slusky, H. Karunadasa, R. J. Cava, and P. Schiffer, *Phys. Rev. B* **69**, 064414 (2004).
- ²⁰ I. A. Ryzhkin, *JETP* **101**, 481 (2005).
- ²¹ L. D. C. Jaubert and P.C.W. Holdsworth, *Nature Physics* **5**, 258 (2009).
- ²² see e.g., C. L. Henley, *Ann. Rev. Cond. Mat. Phys.* **1**, 179 (2010), and references therein.
- ²³ C. Castellano, R. Moessner, and S. L. Sondhi, *Phys. Rev. Lett.* **104**, 107201 (2010).
- ²⁴ R. Siddharthan, B. S. Shastry, A. P. Ramirez, A. Hayashi, R. J. Cava, and S. Rosenkranz, *Phys. Rev. Lett.* **83**, 1854 (1999); B. C. den Hertog and M. J. P. Gingras, *Phys. Rev. Lett.* **84**, 3430 (2000).
- ²⁵ R. G. Melko, B. C. den Hertog, and M. J. P. Gingras, *Phys. Rev. Lett.* **87**, 067203 (2001).
- ²⁶ T. Yavors'kii, T. Fennell, M. J. P. Gingras, and S. T. Bramwell, *Phys. Rev. Lett.* **101**, 037204 (2008).
- ²⁷ P. W. Debye and E. Hückel, *Phys. Z.* **24**, 185 (1923); see Y. Levin, *Rep. Prog. Phys.* **65**, 1577 (2002) for a review on the subject.
- ²⁸ W. Krauth and R. Moessner, *Phys. Rev. B* **67**, 064503 (2003).
- ²⁹ R. G. Melko and M. J. P. Gingras, *J. Phys.: Condens. Matter* **16**, R1277 (2004).
- ³⁰ Note that the slope in the experimental data between, say, 5 and 10 K can be accounted for by higher-energy defects (4in-0out and 4out-0in tetrahedra), which are forbidden in the DH calculations discussed here [see L. D. C. Jaubert and P.C.W. Holdsworth, *J. Phys.: Condens. Matter* **23**, 164222 (2011)].
- ³¹ See for instance M. E. Fisher and Y. Levin, *Phys. Rev. Lett.* **71**, 3826 (1993).
- ³² N. Bjerrum, *Kgl. Dan. Vidensk. Selsk. Mat.-fys. Medd.* **7**, 1 (1926).
- ³³ D. Slobinsky, C. Castellano, R. A. Borzi, A. S. Gibbs, A. P. Mackenzie, R. Moessner, and S. A. Grigera, *Phys. Rev. Lett.* **105**, 267205 (2010).
- ³⁴ S. V. Isakov, R. Moessner, and S. L. Sondhi, *Phys. Rev. Lett.* **95**, 217201 (2005).
- ³⁵ P. Conlon, DPhil Thesis, Oxford University (2010).
- ³⁶ S. Mostame, C. Castellano, R. Moessner, and S. L. Sondhi, (in preparation).